Note on Error Mitigation

Takahiro Yamamoto

June 18, 2019

1 Type of error

Qubit operations are susceptible to various types of errors due to imperfect control pulses, qubit-qubit couplings (crosstalk), and environmental noise. In order to improve qubit performance, it is necessary to identify the types and magnitudes of these errors and reduce them.

1. State preparation and measurement (SPAM)
   (a) intrinsic
   (b) extrinsic
2. Gate infidelity
   (a) 1 qubit operation
   (b) 2 qubit operation

It will be useful to classify SPAM errors into two different types, which we will call *intrinsic* and *extrinsic*. Intrinsic SPAM errors are those that are inherent in the state preparation and measurement process. One example is an error initializing the $|0\rangle$ state due to thermal populations of excited states. Another is dark counts when attempting to measure, say, the $|1\rangle$ state. Extrinsic SPAM errors are those due to errors in the gates used to transform the initial state to the starting state (or set of states) for the experiment to be performed.

Intrinsic SPAM errors are of particular relevance to fault-tolerant quantum computing, since it turns out that quantum error correction (QEC) requirements are much more stringent on gates than on SPAM.

1. Dephasing
2. Amplitude and phasing damping
3. Homogeneous depolarizing

1. Localized Markovian

2. Unbiased statistical fluctuation

Below are some concrete examples of quantum noise and quantum operations. They are also important in understanding the practical effects of noise on quantum systems, and how noise can be controlled by techniques such as error-correction.

Quantum operations can be represented in the operator-sum representation:

$$\mathcal{E}(\rho) = \sum_k E_k \rho E_k^\dagger, \tag{1}$$

where the operators $\{E_k\}$ are known as operation elements.

1.1 Depolarizing

Imagine we take a single qubit, and with probability p that qubit is depolarized. That is, it is replaced by the completely mixed state, $I/2$. With probability $1-p$ the qubit is left untouched. The state of the quantum system after this noise is:

$$\mathcal{E}(\rho) = \frac{pI}{2} + (1-p)\rho \tag{2}$$

In the operator-sum representation,

$$\mathcal{E}(\rho) = \left(1 - \frac{3p}{4}\right)\rho + \frac{p}{4}(X\rho X + Y\rho Y + Z\rho X) \tag{3}$$

1.2 Amplitude damping

the description of energy dissipation-effects due to loss of energy from a quantum system.

$$\mathcal{E}(\rho) = E_0 \rho E_0^\dagger + E_1 \rho E_1^\dagger \tag{4}$$

where

$$E_0 = \begin{bmatrix} 1 & 0 \\ 0 & \sqrt{1-\gamma} \end{bmatrix}, \tag{5}$$

$$E_1 = \begin{bmatrix} 0 & \sqrt{\gamma} \\ 0 & 0 \end{bmatrix}. \tag{6}$$

γ can be thought of as the probability of losing energy. The E_1 operation changes a $|1\rangle$ state into a $|0\rangle$ state, corresponding to the physical process of losing a quantum of energy to the environment. E_0 leaves $|0\rangle$ unchanged, but reduces the amplitude of a $|1\rangle$ state; physically, this happens because a quantum of energy was not lost to the environment, and

thus the environment now perceives it to be more likely that the system is in the $|0\rangle$ state, rather than the $|1\rangle$ state.

$\mathcal{E}_{\mathrm{GAD}}$, called generalized amplitude damping, is defined for single qubits by the operation elements

$$E_0 = \sqrt{p}\begin{bmatrix}1 & 0\\ 0 & \sqrt{1-\gamma}\end{bmatrix}, \tag{7}$$

$$E_1 = \sqrt{p}\begin{bmatrix}0 & \sqrt{\gamma}\\ 0 & 0\end{bmatrix}, \tag{8}$$

$$E_2 = \sqrt{1-p}\begin{bmatrix}\sqrt{1-\gamma} & 0\\ 0 & 1\end{bmatrix}, \tag{9}$$

$$E_3 = \sqrt{1-p}\begin{bmatrix}0 & 0\\ \sqrt{\gamma} & 0\end{bmatrix}. \tag{10}$$

where the stationary state ρ_∞, which statisfies $\mathcal{E}_{\mathrm{GAD}}(\rho_\infty) = \rho_\infty$ is,

$$\rho_\infty = \begin{bmatrix}p & 0\\ 0 & 1-p\end{bmatrix}. \tag{11}$$

When γ is replaced with a time-varying function like $1 - e^{t/T_1}$, you can visualize the effects of amplitude damping as a flow on the Bloch sphere, which moves every point in the unit ball towards a fixed point at $|0\rangle$.

1.3 Phase damping

A noise process that is uniquely quantum mechanical, which describes the loss of quantum information without loss of energy, is phase damping. The energy eigenstates of a quantum system do not change as a function of time, but do accumulate a phase which is proportional to the eigenvalue. When a system evolves for an amount of time which is not precisely known, partial information about this quantum phase – the relative phases between the energy eigenstates – is lost. A phase kick, the angle of rotation θ is random. The randomness could originate, for example, from a deterministic interaction with an environment, which never again interacts with the system and thus is implicitly measured. Let us assume that the phase kick angle θ is well represented as a random variable which has a Gaussian distribution $e^{-\theta^2/4\lambda}$ with mean 0 and variance 2λ.

The random phase kicking causes the expected value of the off-diagonal elements of the density matrix to decay exponentially to zero with time, $e^{-\lambda}$. That is a characteristic result of phase damping.

$$\mathcal{E}(\rho) = E_0\rho E_0^\dagger + E_1\rho E_1^\dagger \tag{12}$$

where

$$E_0 = \begin{bmatrix} 1 & 0 \\ 0 & \sqrt{1-\gamma} \end{bmatrix}, \tag{13}$$

$$E_1 = \begin{bmatrix} 0 & 0 \\ 0 & \sqrt{\gamma} \end{bmatrix}. \tag{14}$$

By applying the unitary freedom of quantum operations, we find that a unitary recombination of E_0 and E_1 gives a new set of operation elements for phase damping;

$$E_0' = \sqrt{\alpha} I \tag{15}$$

$$E_1' = \sqrt{1-\alpha} Z, \tag{16}$$

where $\alpha = (1 + \sqrt{1-\lambda})/2$. Thus the phase damping quantum operation is exactly the same as the phase flip channel.

Phase damping is often referred to as a T_2 relaxation process, for historical reasons, where dephasing time is related to γ as $e^{-t/2T_2} = \sqrt{1-\gamma}$. As a function of time, the amount of damping increases, corresponding to an inwards flow towards σ_z-axis.

1.4 Phase flip

$$\mathcal{E}(\rho) = p\rho + (1-p) Z\rho Z \tag{17}$$

1.5 Bit flip

The bit flip channel flips the state of a qubit from $|0\rangle$ to $|1\rangle$ (and vice versa) with probability $1-p$. It has operation elements

$$\mathcal{E}(\rho) = \sqrt{p} I \rho \sqrt{p} I + \sqrt{1-p} X \rho \sqrt{1-p} X \tag{18}$$

1.6 Bit-phase flip

$$\mathcal{E}(\rho) = \sqrt{p} I \rho \sqrt{p} I + \sqrt{1-p} X \rho \sqrt{1-p} Y \tag{19}$$

2 Error models

2.1 Coherence

The decay time, (T_1) and dephasing time, (T_2)

$$f(t) = Ae^{-t/T_1} + C \tag{20}$$

for unknown parameters A, C, and T_1. If there are no SPAM errors, $A = 1$ and $C = 0$. Similarly, for T_2 and T_2^*, the ground state population is expected to behave like

$$f(t) = Ae^{-t/T_2^*} \cos(2\pi f t + \phi) + C \tag{21}$$

respectively; both with $A = C = 1/2$ in the lack of SPAM errors.

2.2 Hamiltonian Characterization

Measuring ZZ perform an experiment to measure ZZ between a pair of qubits. ZZ here is defined as the energy shift on the $|11\rangle$ state,

$$H = \frac{\omega_0}{2}(1 - \sigma_{Z,0}) + \frac{\omega_1}{2}(1 - \sigma_{Z,1}) + \xi \left|11\right\rangle \left\langle 11\right| \tag{22}$$

The experiment to measure ξ is to perform a Ramsey experiment on Q0 (H-t-H) and repeat the Ramsey with Q1 in the excited state. The difference in frequency between these experiments is the rate ξ. ZZ rates are typically ≈100kHz so we want Ramsey oscillations around 1MHz. 12 numbers ranging from 10 to 1000, logarithmically spaced

2.3 Amplitude Error Characterization for Single Qubit Gates

Measure the amplitude error in the single qubit gates. Here this measures the error in the $\pi/2$ pulse. Note that we can run multiple amplitude calibrations in parallel. This shows the sequence of the calibration, which is repeated application of Y_π ($U_2(0, 0)$). Note that the measurements are mapped to a minimal number of classical registers in order of the qubit list.

Suppose error model where each Y_π gate has error

$$\begin{bmatrix} \cos(\theta) & -\sin(\theta) \\ \sin(\theta) & \cos(\theta) \end{bmatrix}. \tag{23}$$

Excited state population can be fit as:

$$C - \frac{1}{2}\cos\left[\left(\theta + \frac{\pi}{2}\right)(x + 1)\right] \tag{24}$$

where x is the number of gate repetitions and θ is the error for the pulse (amplitude/error). [TODO: fill the gap]

2.4 Angle Error Characterization for Single Qubit Gates

Measure the angle between the X and Y gates

Gate sequence for measuring the angle error $U_2(0, 0)U_1(2\theta)U_2(-\pi/2, \pi/2)U_2(-\pi/2, \pi/2) \cdots$ where the U_1 gates are added errors to test the procedure

2.5 Amplitude Error Characterization for CNOT Gates

This looks for a rotation error in the CNOT gate, ie., if the gate is actually $CR_X(\pi/2+\delta)$ measure δ. This is very similar to the single qubit amplitude error calibration except we need to specify a control qubit (which is set to be in state $|1\rangle$) and the rotation is a π.

Suppose error model where each CNOT gate has error

$$\begin{bmatrix} 1 & 0 & 0 & 0 \\ 0 & 1 & 0 & 0 \\ 0 & 0 & \cos(\theta) & -i\sin(\theta) \\ 0 & 0 & -i\sin(\theta) & \cos(\theta) \end{bmatrix}. \tag{25}$$

$$C + \frac{1}{2}\sin\left[(\theta+\pi)\,x\right] \tag{26}$$

where x is the number of gate repetitions and θ is the amplitude error for the pulse. See: [https://qiskit.org/documentation/ignis/characterization.html]

2.6 Angle Error Characterization for CX Gates

Measure the angle error θ in the CNOT gate, i.e., $CR_{\cos(\theta)X+\sin(\theta)Y}(\pi/2)$ with respect to the angle of the single qubit gates.

2.7 Error models

$$\Lambda(\rho) = \sum_k E_k \rho E_k^\dagger \tag{27}$$

$$E_1 = \frac{1+\sqrt{1-\gamma-\lambda}}{2} I + \frac{1-\sqrt{1-\gamma-\lambda}}{2} Z \tag{28}$$

$$E_2 = \frac{\sqrt{\gamma}}{2}(X+iY) \tag{29}$$

$$E_1 = \frac{\sqrt{\lambda}}{2}(I-Z) \tag{30}$$

$$\Lambda(\rho) \to \sum_{A\in\mathcal{A}} A^\dagger \Lambda(A\rho A^\dagger) A = \sum_{A\in\mathcal{A}} p_A A^\dagger \rho A \tag{31}$$

$$\mathcal{A} = \{I, X, Y, Z\} \tag{32}$$

3 Qubit characterization methods

Several methods of qubit characterization are currently available[1]. In chronological order of their development, the main techniques are:

1. quantum state tomography (QST)
2. quantum process tomography (QPT)
3. randomized benchmarking (RB)
4. quantum gate set tomography (GST)

3.1 Quantum state tomography (QST)

3.2 Quantum process tomography (QPT)

A quantum operation on a d-dimensional quantum system can be completely determined by experimentally measuring the output density matrices produced from d^2 pure state inputs.

3.3 Randomized benchmarking (RB)

3.4 Quantum gate set tomography (GST)

GST arose from the observation that QPT is inaccurate in the presence of SPAM errors. In QPT, the starting states must form an informationally complete basis of the Hilbert-Schmidt space on which the gate being estimated acts. These are typically created by applying gates to a given initial state, usually the $|0\rangle$ state, and these gates themselves may be faulty.

According to recent results from IBM, a 50-fold increase in intrinsic SPAM error reduces the surface code threshold by only a factor of 3-4. Therefore QPT – the accuracy of which degrades with increasing SPAM – would not be able to determine if a qubit meets threshold requirements when the ratio of intrinsic SPAM to gate error is large.

This is not an issue for extrinsic SPAM errors, which go to zero as the errors on the gates go to zero. Nevertheless, extrinisic SPAM error interferes with diagnostics: as an example, QPT cannot distinguish an over-rotation error on a single gate from the same error on all gates. In addition, Merkel, et al. have found that, for a broad range of gate error – including the thresholds of leading QEC code candidates – the ratio of QPT estimation error to gate error increases as the gate error itself decreases. This makes QPT less reliable as gate quality improves.

Extrinsic SPAM error is also unsatisfactory from a theoretical point of view: QPT assumes the ability to perfectly prepare a complete set of states and measurements. In

[1] Introduction to Quantum Gate Set Tomography, D. Greenbaum, arXiv:1509.02921

reality, these states and measurements are prepared using the same faulty gates that QPT attempts to characterize. One would like to have a characterization technique that takes account of SPAM gates self-consistently. We shall see that GST is able to resolve all of these issues.

Another approach to dealing with SPAM errors is provided by randomized benchmarking. RB is based on the idea of twirling – the gate being characterized is averaged in a such a way that the resulting process is depolarizing with the same average fidelity as the original gate. The depolarizing parameter of the averaged process is measured experimentally, and the result is related back to the average fidelity of the original gate. This technique is independent of the particular starting state of the experiment, and therefore is not affected by SPAM errors. However, RB has several shortcomings which make it unsatisfactory as a sole characterization technique for fault-tolerant QIP. For one thing, it is limited to Clifford gates, and so cannot be used to characterize a universal gate set for quantum computing. For another, RB provides only a single metric of gate quality, the average fidelity. This can be insufficient for determining the correct qubit error model to use for evaluating compatibility with QEC. Several groups have shown that qualitatively different errors can produce the same average gate fidelity, and in the case of coherent errors the depolarizing channel inferred from the RB gate fidelity underestimates the effect of the error. Finally, RB assumes the errors on subsequent gates are independent. This assumption fails in the presence of non-Markovian, or time-dependent noise. GST suffers from this assumption as well, but the long sequences used in RB make this a more pressing issue.

Despite these apparent shortcomings, RB has been used with great success by several groups to measure gate fidelities and to diagnose and correct errors. RB also has the advantage of scalability – the resources required to implement RB (number of experiments, processing time) scale polynomially with the number of qubits being characterized. QPT and GST, on the other hand, scale exponentially with the number of qubits. As a result, these techniques will foreseeably be limited to addressing no more than 2-3 qubits at a time.

GST and RB may end up complementing each other as elements of a larger characterization protocol for any future multi-qubit quantum computer.

TODO: summarize them in table.

method	assumption	advantage	disadvantage	scalability
quantum state tomography				
quantum process tomography				
randomized benchmarking				
quantum gate set tomography				

4 Type of error mitigation technics

There are four types of errors that can result in infidelity in the variational quantum simulation:

1. errors due to limited generality of the trial wave function, which may only be able to describe the simulated system approximately;
2. shot noise (TODO: definition) in measurments
3. errors due to noise in the quantum machine, e.g., decoherence and quantum gate infidelity.

Type of error mitigation technics are listed as:

1. Error extrapolation
2. Quasiprobability decomposition
3. Quantum subspace expansion. quantum channels
4. Process tomography protocols
   (a) Gate set tomography

4.1 Homogeneous and inhomogeneous scaling

4.1.1 Theory

Consider the case in which the effect of machine noise is to depolarize the ancillary qubit at a fixed level; *i.e.*, the output of the quantum computer becomes $\langle X \rangle = \eta \langle X \rangle^{(0)}$, where η is a constant independent of the quantum circuit.

An example of the homogeneous scaling is the case of balanced measurement errors. Errors in the measurement on the ancillary qubit (see Fig.?) can be modeled as follows:

1. If the state of the qubit is $|0\rangle$ the measurement outcome is correct with the probability $(1 - p_0)$ and the outcome is incorrect with the probability p_0
2. If the state of the qubit is $|1\rangle$ the measurement outcome is correct with the probability $(1 - p_1)$ and the outcome is incorrect with the probability p_1

Then the expectation value is $\langle X \rangle = (p_1 - p_0) + (1 - p_0 - p_1) \langle X \rangle^{(0)}$,

If measurement errors are balanced, *i.e.*, $p_0 = p_1$, the effect of measurement errors is a fixed scaling factor $\eta = 1 - p_0 - p_1$, which does not result in computing errors. Therefore, the hybrid algorithm is inherently insensitive to measurement errors on the ancillary qubit if these errors are balanced. Note also that if single-qubit gates are reliable, one can flip

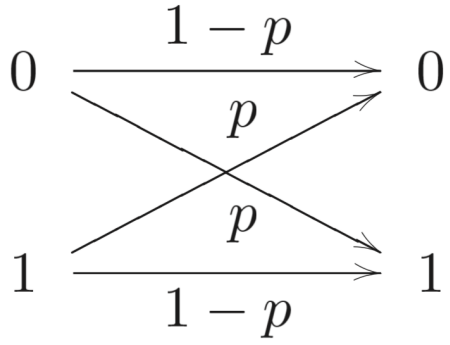

the qubit before the measurement so that measurement errors are effectively balanced. Measurement errors can be corrected even if they are not balanced. If p_0 and p_1 can be evaluated by benchmarking measurement operations, one can easily work out the true value $\langle X\rangle^{(0)}$ using the value obtained from the real machine: $\langle X\rangle^{(0)} = [\langle X\rangle - (p_1 - p_0)]/(1 - p_0 - p_1)$ We note that when error probabilities are higher, the denominator is smaller, which means that we need to evaluate $[\langle X\rangle$ with a higher accuracy in order to achieve the same accuracy of $\langle X\rangle^{(0)}$[2]

4.1.2 Experiment

4.1.3 Summary

4.2 Error extrapolation

4.2.1 Motivation

4.2.2 Theory

Errors in an operation are stochastic if the operation is described by a superoperator $\mathcal{NU}$ and $\mathcal{N}$ has the form $\mathcal{N} = (1 - \epsilon)\mathcal{I} + \mathcal{E}$. Here, $\mathcal{U}$ is the ideal operation without errors, $\mathcal{N}$ is the superoperator describing the effect of the noise, $\mathcal{I}$ is an identity operation, and errors $\mathcal{E}$ occur with the probability ϵ. Here, $\mathcal{E}$ is a valid quantum operation, *i.e.*, trace-preserving completely positive map.

Given an initial state ρ, after a sequence of operations, the final state of the quantum computer is $\rho = \mathcal{N}_L\mathcal{U}_L \cdots \mathcal{N}_\ell\mathcal{U}_\ell \cdots \mathcal{N}_1\mathcal{U}_1\rho$

where $\mathcal{N}_\ell\mathcal{U}_\ell$ denotes the ℓ-th operation. Taking into account the fact that errors are stochastic, the outcome can be rewritten in the form

$$\langle X\rangle = \left(1 - r\sum \epsilon_\ell\right)\langle X\rangle^{(0)} + r\langle X\rangle^{(1)} + \mathcal{O}(r^2), \tag{33}$$

[2] PhysRevX.7.021050

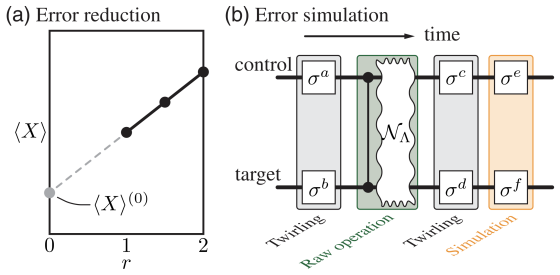

where r is a convenient scale factor. For more detailed discussion see [PhysRevX.7.021050]. If probabilities of errors are tunable, we can infer the value of $\langle X \rangle^{(0)}$ by measuring values of $\langle X \rangle$ of a set of different factors r [see Fig.?].

To infer the value of $\langle X \rangle^{(0)}$, first, we take N_X values of r and measure $\langle X \rangle$ with $r_1, \cdots, r_X$, where we can take $r_1 = 1$. Then, we fit the output as $\langle X \rangle (r) = \langle X \rangle^{(0)} + \chi r$ and obtain the value of $\langle X \rangle^{(0)}$. In this way, the first-order contribution of machine noise can be corrected. Similarly, by considering second-order terms in the expansion Eq.?, we can fit data using a function with second-order terms.

Using the extrapolation, we can reduce the effect of the machine noise. However, the final estimation of $\langle X \rangle^{(0)}$ may still be different from its actual value, and the error in the extrapolation depends on the shot noise in estimating each $\langle X \rangle (r)$.

The error-reduction protocol only works for small-size circuits, which are used in the hybrid algorithm, while the Trotterization algorithm usually needs large-size circuits. The true value $\langle X \rangle^{(0)}$ can be inferred when the contribution of high-order terms is much smaller than the contribution of lower-order terms.

The total rate of errors in the circuit with N_g gates is approximately $1 - (1 - \epsilon)^{N_g} = N_g\epsilon + (N_g\epsilon)^2/2 + \cdots$.

When there are too many gates in the circuit or the error rate is too high, $N_g\epsilon \gtrapprox 1$, the quantum state will be populated with errors, and one cannot retrieve the true value $\langle X \rangle^{(0)}$ even if we consider high-order terms in the interpolation.

4.2.3 Experiment

4.2.4 Summary

4.3 Error twirling

TODO: fill in

4.4 Quasiprobability decomposition

4.4.1 Motivation

4.4.2 Theory

Utility of "twirling" operations in minimizing the cost[3]. For the extrapolation method, their optimisation is to observe that typically for the classes of noise most common in experiments it is appropriate to assume that the expected values of the observation will decay exponentially with he severity of the circuit noise, rather than polynomial.

4.4.3 Experiment

4.4.4 Summary

4.5 Process tomography protocols

Localized Markovian errors

4.5.1 Motivation

4.5.2 Theory

Single-qubit Clifford gates and measurements are universal in computing expectation values. Any quantum operation is a linear map. Single qubit Clifford gates and measurements yield a complete set of linear independent maps. Any error can be simulated or subtracted by decomposition of the error using complete operation set.

By combining GST and the complete set decomposition, any localized Markovian errors in the QC can be systematically mitigated, so that the error in the final computational output is due to unbiased statistical fluctuation.

4.5.3 Experiment

4.5.4 Summary

5 Summary

1. Error mitigation method
2. Applicable error type
3. Efficiency
4. Cost (per qubit)

[3]Error Mitigation for Short-Depth Quantum Circuits, K. Temme, S. Bravyi, and J. M. Gambetta, Phys. Rev. Lett. 119, 180509

A Topological QC

Fault-tolerant quantum computing can be achieved by encoding qubits in non-Abelian anyons in topological materials[4]

B Quantum error correction

However, quantum error correction involves a substantial multiplication of resources; the number of physical qubits required may be orders of magnitude greater than the number of error-free logical qubits seen by the algorithm. A recent study audited the cost of implementing Shor's algorithm to solve a classically infeasible task and found that, even with state-of-the-art techniques for magic-state distillation, the machine would need over six million of today's highest- quality qubits[5].

C Dynamics simulation of quantum system

Dynamics must be studied when properties cannot be determined from static features. This has motivated dynamical versions of many well-known techniques, e.g., nonequilibrium dynamical mean-field theory[6], the time-dependent variational quantum Monte Carlo method[7], time-dependent tensor network methods[8], and, of course, time-dependent density functional theory[9].

A new approach[10] is based on the variational method, and our hope is that it could be implemented using small- size quantum circuits, i.e., quantum circuits with a small number of quantum operations that suffer significant noise compared with fault-tolerant quantum computers.

Variational methods have numerous applications in the numerical study of many-body

[4] A. Kitaev, Fault-Tolerant Quantum Computation by Anyons, Ann. Phys. (Amsterdam) 303, 2 (2003).

[5] J. O'Gorman and E. T. Campbell, Quantum Computation with Realistic Magic State Factories, Phys. Rev. A 95, 032338 (2017)

[6] H. Aoki, N. Tsuji, M. Eckstein, M. Kollar, T. Oka, and P. Werner, Nonequilibrium Dynamical Mean-Field Theory and Its Applications, Rev. Mod. Phys. 86, 779 (2014).

[7] G. Carleo, F. Becca, M. Schiro, and M. Fabrizio, Localization and Glassy Dynamics of Many-Body Quantum Systems, Sci. Rep. 2, 243 (2012).

[8] A. J. Daley, C. Kollath, U. Schollwock, and G. Vidal, Time-Dependent Density-Matrix Renormalization-Group Using Adaptive Effective Hilbert Spaces, J. Stat. Mech. (2004) P04005., M. C. Banuls, M. B. Hastings, F. Verstraete, and J. I. Cirac, Matrix Product States for Dynamical Simulation of Infinite Chains, Phys. Rev. Lett. 102, 240603 (2009).

[9] E. Runge and E. K. U. Gross, Density-Functional Theory for Time-Dependent Systems, Phys. Rev. Lett. 52, 997 (1984).

[10] Ying Li and Simon C. Benjamin, Efficient Variational Quantum Simulator Incorporating Active Error Minimization, Physical Review X 7, 021050 (2017)

quantum systems: for example, density functional theory[11], the matrix product state method[12], and simulating molecular dynamics using the variational principle[13]

[11]R. O. Jones, Density Functional Theory: Its Origins, Rise to Prominence, and Future, Rev. Mod. Phys. 87, 897 (2015).

[12]D. Perez-Garcia, F. Verstraete, M. M. Wolf, and J. I. Cirac, Matrix Product State Representations, Quantum Inf. Comput. 7, 401 (2007).

[13]H. Feldmeier and J. Schnack, Molecular Dynamics for Fermions, Rev. Mod. Phys. 72, 655 (2000).